Optics Communications 96 (1993) 150–163
North-Holland

OPTICS
COMMUNICATIONS

Full length article

Central resonance of the Mollow absorption spectrum: physical origin of gain without population inversion

Gilbert Grynberg
Laboratoire de Spectroscopie Hertzienne de l'Ecole Normale Supérieure, Case 74, Université Pierre et Marie Curie, F-75252 Paris Cedex 05, France

and

Claude Cohen-Tannoudji
Collège de France and Laboratoire de Spectroscopie Hertzienne de l'ENS, Département de Physique de l'ENS, 24 rue Lhomond, F-75231 Paris Cedex 05, France

Received 17 July 1992

The physical origin of the central resonance of the Mollow absorption spectrum for a two-level atom is studied. This resonance has a dispersive line shape and is centered in $\omega'=\omega$ where ω' and ω are the frequencies of the probe and pump beam. We give a diagrammatic interpretation of this resonance and we show that it is associated with two-photon spontaneous emission processes. The amplification of the weak beam can be described by one amplitude which exhibits a resonance in $\omega=\omega'$. On the other hand, the absorption is described by two amplitudes, one resonant and one nonresonant. The resonant amplification and absorption amplitudes have effects which are balanced. The interference between the resonant and nonresonant absorption amplitudes breaks this symmetry and permits to achieve amplification. This is an example of gain without population inversion because the transition occurs between equally populated levels both in the bare and dressed atom basis. Examples of lasers working along this scheme have indeed been reported in the literature. We finally show that these ideas can be used to suggest new types of lasers without population inversion.

1. Introduction

The absorption spectrum of a weak probe beam of frequency ω' by a two-level atom submitted to an intense pump wave of frequency ω has been calculated by Mollow in 1972 [2] and observed [1] a few years later. This spectrum consists of three lines (fig. 1a). When the intense beam is detuned from resonance and when its intensity is not too large, these lines are centered in ω_0, $2\omega-\omega_0$ and ω where ω_0 is the atomic frequency. The resonance in $\omega'\approx\omega_0$ corresponds to a resonant elastic scattering process where one probe photon ω' is absorbed and one fluorescence photon with frequency $\omega_1=\omega'$ is emitted (fig. 1b). The resonance in $\omega'\approx 2\omega-\omega_0$ corresponds to a higher-order scattering process where two pump photons ω are absorbed and two photons are emitted, one stimulated photon at frequency ω' and one spontaneous photon at frequency $\omega_2\approx\omega_0$ (fig. 1c). This scattering process has been widely studied in the literature for its applications to spectroscopy [3] and amplification of field ω' [4]. In contrast with the resonances occurring in ω_0 and $2\omega-\omega_0$ which have a clear physical interpretation, the dispersion line centered in $\omega'=\omega$ is not so easy to understand. Detailed calculations using optical Bloch equations have been done [5–7] and have shown good agreement with experimental studies [6]. Macroscopic descriptions have also been derived which involve grating formations [8] or time-modulated excitation [9]. The connection with two-wave mixing in photo refractive crystals and stimulated Rayleigh scattering has also been stressed [8]. However no microscopic description showing how photons are exchanged

0030-4018/93/$ 06.00

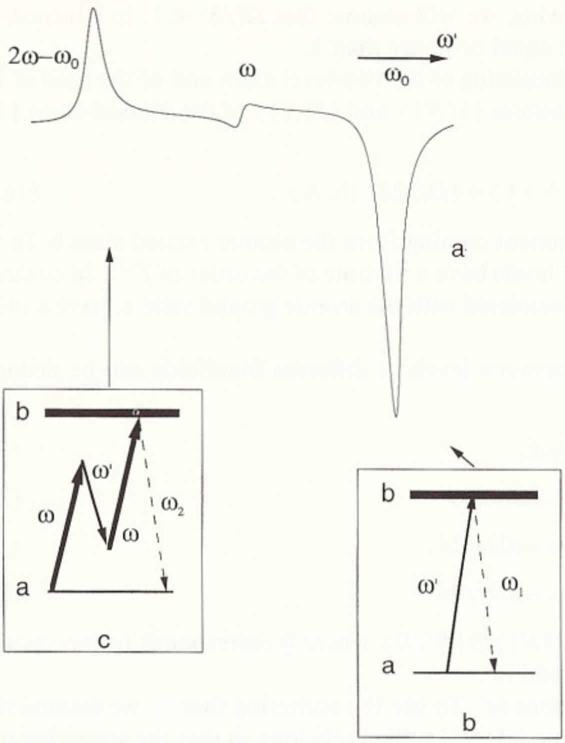

Fig. 1. (a) Sketch of the variations with ω' of the intensity of a weak probe beam of frequency ω' transmitted through a gas of two-level atoms (atomic frequency ω_0) interacting with an intense pump beam of frequency ω. (b) Rayleigh scattering process at the origin of the absorption line of (a), centered in $\omega' \approx \omega_0$: absorption of one probe photon ω' and spontaneous emission of one fluorescence photon ω_1. Pump photons are represented with thick arrows, probe photons with thin arrows and fluorescence photons with dashed arrows. Level b is represented with a thick line to describe its natural width Γ, whereas the stable level a is represented with a thin line. (c) Multiphoton process at the origin of the amplification line of (a), centered in $\omega' \approx 2\omega - \omega_0$: absorption of one pump photon ω, stimulated emission of one probe photon ω', absorption of a second pump photon ω, and, finally, spontaneous emission of one fluorescence photon ω_2. The spectrum of (a) exhibits also a small dispersion-like structure near $\omega' \approx \omega$, the interpretation of which is the subject of this paper.

near this resonance between the fields and the atom has, to our knowledge been proposed so far. This is the aim of this paper. We will show that the dispersive shape involves the competition between gain and absorption processes for photons ω'. Two fluorescence photons appear in the diagrams describing these processes. The absorption process involves the interference between several amplitudes, some of them involving a resonance for $\omega' \approx \omega$. Depending upon the sign of $\omega - \omega'$, the interference is destructive (absorption decreases) or constructive (absorption increases). Note that a similar interference does not exist for the gain. Because of the interference appearing on the absorption, gain and absorption are not balanced and an amplification of the weak beam may be obtained. A laser based on this amplification process has indeed worked [8,10]. Since this amplification scheme does not involve any population inversion (neither in the bare atom basis nor in the dressed atom basis [11]), the present study is also connected with the problem of laser without population inversion [12] which has recently attracted a considerable attention.

2. General

We consider a two-level atom (ground state a, excited state b having a lifetime Γ^{-1}) interacting with two quasiresonant fields of frequencies ω and ω'. The detunings from resonance $\delta = \omega - \omega_0$ and $\delta' = \omega' - \omega_0$ verify $\Gamma \ll |\delta|, |\delta'| \ll \omega$. However, we assume that $\omega - \omega'$ remains on the order of Γ so that $|\omega - \omega'| \ll |\delta|, |\delta'|$. We use a quantum description for the fields and assume that initially there are N photons in the mode ω, N' photons in the mode ω' ($N \gg N' \gg 1$) and that the other modes are empty. The resonance Rabi frequency for the two-level atom interacting with the field ω is $\Omega_1 = -d\sqrt{2\omega/\epsilon_0 \hbar}\sqrt{N/L^3}$ where L^3 is the quantization volume and d is the matrix element of the electric dipole moment assumed to be real ($d = \langle \mathrm{b} | \boldsymbol{d} \cdot \boldsymbol{e}_z | \mathrm{a} \rangle$ where $\boldsymbol{e}_z$ is the polarization of the fields ω and ω') [11]. In the following, we will assume that $\Omega_1^2/\delta^2 \ll 1$. In contrast, no assumption is made for $\Omega_1^2/\Gamma|\delta|$ which can possibly be equal or larger than 1.

We use a dressed-state representation for the system consisting of the two-level atom and of the field of frequency ω. In the limit $\Omega_1/|\delta| \ll 1$ and for $\delta < 0$, the eigenstates $|1(N)\rangle$ and $|2(N)\rangle$ of the dressed-atom [11] are respectively equal to:

$$|1(N)\rangle = |\mathrm{b}, N\rangle - (\Omega_1/2\delta)\ |\mathrm{a}, N+1\rangle\ , \quad |2(N)\rangle = |\mathrm{a}, N+1\rangle + (\Omega_1/2\delta)\ |\mathrm{b}, N\rangle\ . \tag{1a,b}$$

We note that the $|1(N)\rangle$ levels have a dominant component coming from the atomic excited state b. In the radiative cascade of the dressed-atom [11], the $|1(N)\rangle$ levels have a lifetime of the order of Γ^{-1}. In contrast, the levels $|2(N)\rangle$ which have a dominant component associated with the atomic ground state a, have a much longer lifetime

The matrix elements of the electric dipole moment between levels of different manifolds can be deduced from eq. (1):

$$d_{12}^{+} = \langle 1(N+1) | d | 2(N) \rangle = d_{21}^{-} = \langle 2(N) | d | 1(N+1) \rangle = d\ , \tag{2a}$$

$$d_{22}^{+} = \langle 2(N+1) | d | 2(N) \rangle = d_{22}^{-} = \langle 2(N) | d | 2(N+1) \rangle = d\Omega_1/2\delta\ , \tag{2b}$$

$$d_{11}^{+} = \langle 1(N+1) | d | 1(N) \rangle = d_{11}^{-} = \langle 1(N) | d | 1(N+1) \rangle = -d\Omega_1/2\delta\ , \tag{2c}$$

$$d_{21}^{+} = \langle 2(N+1) | d | 1(N) \rangle = d_{12}^{-} = \langle 1(N) | d | 2(N+1) \rangle = -d\Omega_1^2/4\delta^2\ . \tag{2d}$$

The initial state of the system is assumed to be $|\mathrm{i}\rangle = |2(N)\rangle \otimes |N', 0\rangle$ where 0 corresponds to the vacuum state for all the modes of the field except the modes ω and ω'.

We will study several scattering processes for the photons ω'. To use the scattering theory, we assume that a system in the $|2(N)\rangle$ state does not decay during a time interval sufficiently long so that the scattering process can entirely take place during this interval. Under these conditions, the states $|2(N)\rangle$ can be used as satisfactory asymptotic states for the initial and final states of the scattering process. On the other hand, the levels $|1(N)\rangle$ which have a radiative lifetime on the order of Γ^{-1} cannot be considered as possible final states for a scattering process. Any scattering process considered in this paper should thus start from a $|2(N)\rangle$ level and end in a $|2(N')\rangle$ level. In some sense, this means that the frequency resolution that we consider in the following is on the order of the inverse of the lifetime of the $|2(N)\rangle$ levels (ref. [13], sect. $\mathrm{B_{IV}}$.3).

We will give diagrammatic representations of the scattering processes in the dressed-atom energy diagram. Because several intermediate states can be considered for each scattering process, we split in the corresponding figure the scattering process into different contributions corresponding to different intermediate states. The relevant intermediate states will be represented with solid lines while other levels are shown with dashed lines. In the energy diagram, we will use for the $|1(N)\rangle$ and $|2(N)\rangle$ levels thick and thin lines, respectively. The use of thick lines for the $|1(N)\rangle$ levels is justified by the fact that these levels have a width on the order of Γ because of spontaneous emission. The levels $|2(N)\rangle$ have a much longer lifetime and are assumed to be stable for the scattering processes considered here.

3. Absorption of photons ω'

3.1. Processes involving spontaneous emission of one photon

We first consider the elastic scattering process where one photon ω' is absorbed and one photon is emitted in another mode ω_1. Final states for this process are thus $|2(N)\rangle \otimes |(N'-1), 1\omega_1\rangle$. There are two diagrams which describe this process, each of them being split in two because of different intermediate states. These diagrams are shown in fig. 2. We calculate here the transition amplitude [11] associated with the dominant diagram (fig. 2a). The contribution of the other diagrams is considered in the appendix where it is shown that they can be neglected.

The diagram of fig. 2a corresponds to the absorption of one photon ω' followed by the spontaneous emission of one photon ω_1, the intermediate state of the scattering process being $|1(N+1)\rangle \otimes |(N'-1), 0\rangle$. Using the $-\boldsymbol{d}\cdot\boldsymbol{E}(0)$ interaction hamiltonian between the atom and the field, one finds the transition amplitude $\mathcal{T}_{\mathrm{fi}}^{(2a)}$:

$$\mathcal{T}_{\mathrm{fi}}^{(2a)} = \frac{\sqrt{\omega'\omega_1}}{2\epsilon_0 L^3}\sqrt{N'}\,\epsilon_{1z}\frac{d_{21}^{-}d_{12}^{+}}{\delta'+\mathrm{i}\Gamma/2}, \tag{3a}$$

where ϵ_{1z} is the component of the polarization of the scattered photon along the z direction. Using the $d_{ij}^{\pm}$ of eq. (2a), eq. (3a) yields:

$$\mathcal{T}_{\mathrm{fi}}^{(2a)} = \frac{\sqrt{\omega'\omega_1}}{2\epsilon_0 L^3}\sqrt{N'}\,\epsilon_{1z}\frac{d^2}{\delta'+\mathrm{i}\Gamma/2}. \tag{3b}$$

From the transition amplitude $\mathcal{T}_{\mathrm{fi}}^{(2a)}$, one can calculate the transition rate towards the group of final states $|\mathrm{f}\rangle$ having the same energy as $|\mathrm{i}\rangle$:

$$\sum_{\mathrm{f}} w_{\mathrm{fi}}^{(1)} = \frac{2\pi}{\hbar}\int\frac{\mathrm{d}^3k_1}{(2\pi/L)^3}\sum_{\epsilon_1}|\mathcal{T}_{\mathrm{fi}}^{(2a)}|^2\,\delta(\hbar\omega'-\hbar\omega_1). \tag{4}$$

The total cross-section $\sigma_{\mathrm{abs}}^{(1)}$ for this process is obtained by dividing the transition rate by the flux of photons ω' equal to $N'c/L^3$:

$$\sigma_{\mathrm{abs}}^{(1)} = \frac{L^3}{N'c}\sum_{\mathrm{f}} w_{\mathrm{fi}}^{(1)}. \tag{5}$$

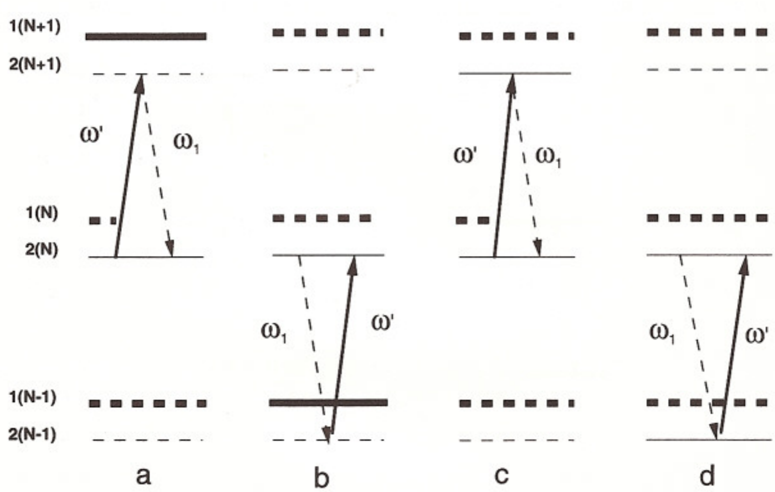

Fig. 2. Diagrammatic representation of the various physical processes involving one fluorescence photon ω_1 and responsible for the absorption of the probe field ω' for $\omega'\approx\omega$. The states $|1(N+1)\rangle$, $|2(N+1)\rangle$, $|1(N)\rangle$, $|2(N)\rangle$, $|1(N-1)\rangle$, $|2(N-1)\rangle$, ..., are the energy levels of the atom dressed by the pump photons ω. For each of the four diagrams, the initial, intermediate and final states of the scattering process are represented with solid lines, whereas the other states are represented with dashed lines. Levels $|1(N+1)\rangle$, $|1(N)\rangle$, $|1(N-1)\rangle$, ..., which contain a large admixture of the atomic excited state b, have a width on the order of the natural width Γ and are represented with thick lines. Levels $|2(N+1)\rangle$, $|2(N)\rangle$, $|2(N-1)\rangle$, ..., are represented with thin lines, because they contain a large admixture of the ground state a, which explains their small radiative width.

Using eqs. (3b) and (4), the relation:

$$d^2=3\pi\epsilon_0\hbar\Gamma(c/\omega_0)^3 \tag{6}$$

and the sum over the polarizations and solid angle [11]:

$$\int \mathrm{d}\Omega_1 \sum_{\epsilon_1} |\epsilon_{1z}|^2=8\pi/3\,, \tag{7}$$

one finds the well known result for the resonant scattering cross-section:

$$\sigma_{\text{abs}}^{(1)}=\frac{3}{2\pi}\lambda_0^2\frac{(\Gamma/2)^2}{\delta'^2+(\Gamma/2)^2}\,, \tag{8}$$

where we have replaced the slowly varying functions of ω' by their value in ω_0. The scattering cross-section $\sigma_{\text{abs}}^{(1)}$ is resonant for $\omega'=\omega_0$ and is associated with the process shown in fig. 1b. Actually, in the situation considered in this paper ($\Gamma\ll|\delta'|\ll\omega$), one deals with the wings of the absorption line. In this condition, we obtain:

$$\sigma_{\text{abs}}^{(1)}\approx(3/8\pi)\lambda_0^2(\Gamma/\delta)^2\,, \tag{9}$$

where we have replaced δ' by δ because $|\delta-\delta'|\ll|\delta|$.

3.2. Processes involving spontaneous emission of two photons

In this section, we consider the transition from $|\mathrm{i}\rangle=|2(N)\rangle\otimes|N',0\rangle$ towards $|\mathrm{f}\rangle=|2(N-1)\rangle\otimes|(N'-1),1\omega_1,1\omega_2\rangle$ where two spontaneous photons are emitted. We first consider the case where ω_1 and ω_2 are close to $(2\omega-\omega_0)$ and ω_0, respectively. We have shown in fig. 3 the dominant diagrams for this scattering process. Two types of diagrams can be distinguished: diagrams (3a) and (3c) have a nonresonant intermediate step while all the steps are nearly-resonant for diagrams (3b), (3d) and (3e). However, the matrix elements of the

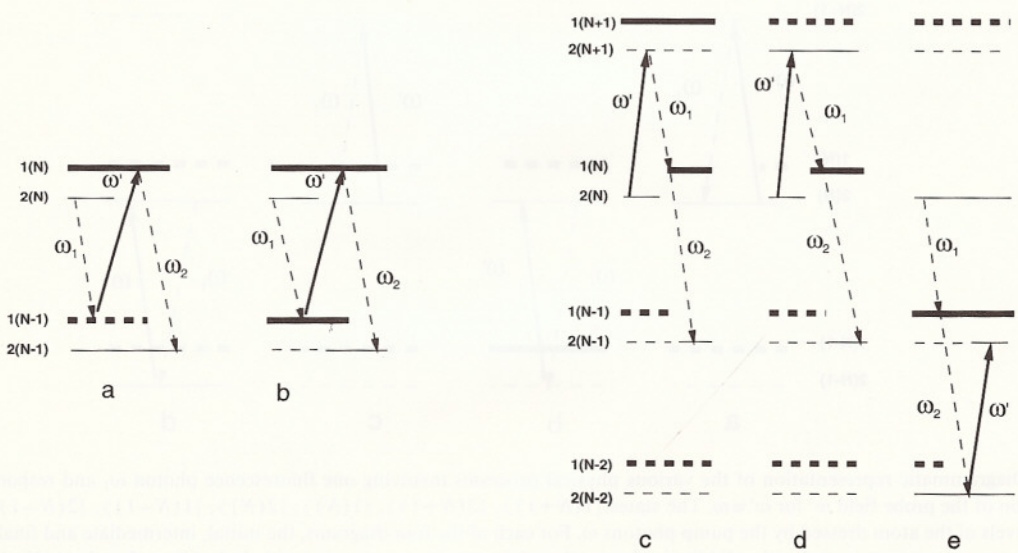

Fig. 3. Diagrammatic representation of the dominant scattering processes, involving two fluorescence photons ω_1 and ω_2 (with $\omega_1\approx2\omega-\omega_0$ and $\omega_2\approx\omega_0$), and responsible for the absorption of the probe field ω', for $\omega'\approx\omega$. The conventions are the same as for fig. 2. Diagrams (a) and (c) contain a non resonant intermediate state, whereas all intermediate states are nearly resonant for diagrams (b), (d), (e).

electric dipole moment are smaller for the nearly-resonant processes. In fact, we will show that the ratio between the transition amplitudes of the resonant and nonresonant processes is on the order of $(\Omega_1^2/\delta^2)(\delta/\Gamma)$. For small values of $\Omega_1^2/\delta\Gamma$, the nonresonant processes are dominant while in the opposite case, the nearly-resonant processes have the largest transition amplitude. Interference effects between all these diagrams should appear in the calculation of the transition rate because the initial and final states of the scattering process are identical.

We first calculate the transition amplitudes associated with the nonresonant processes. For the diagram in fig. 3a, the intermediate states are $|2(N-1)\rangle\otimes|N', 1\omega_1\rangle$ and $|1(N)\rangle\otimes|(N'-1), 1\omega_1\rangle$. The transition amplitude $\mathscr{T}_{\rm fi}^{(3a)}$ is equal to:

$$\mathscr{T}_{\rm fi}^{(3a)}=C\frac{d_{21}^{-}d_{12}^{+}d_{22}^{-}}{[(\omega+\omega'-\omega_1-\omega_0)+\mathrm{i}\Gamma/2](\omega-\omega_1)}, \tag{10}$$

with

$$C=\mathrm{i}\frac{\sqrt{\omega'\omega_1\omega_2}\sqrt{N'}}{(2\epsilon_0L^3)^{3/2}\sqrt{\hbar}}\epsilon_{1z}\epsilon_{2z}. \tag{11}$$

Using $(\omega-\omega_1)\approx[\omega-(2\omega-\omega_0)]=-\delta$ and eqs. (2), we find:

$$\mathscr{T}_{\rm fi}^{(3a)}=C\left(-\frac{\Omega_1}{2\delta}\right)\frac{d^3}{[(\omega+\omega'-\omega_1-\omega_0)+\mathrm{i}\Gamma/2]\delta}. \tag{12}$$

For the diagram in fig. 3c, the intermediate states are $|1(N+1)\rangle\otimes|(N'-1), 0\rangle$ and $|1(N)\rangle\otimes|(N'-1), 1\omega_1\rangle$. One obtains

$$\mathscr{T}_{\rm fi}^{(3c)}=C\frac{d_{21}^{-}d_{11}^{-}d_{12}^{+}}{[(\omega+\omega'-\omega_1-\omega_0)+\mathrm{i}\Gamma/2](\omega'-\omega_0)}. \tag{13}$$

Using $(\omega'-\omega_0)\approx\delta$ and eqs. (2), we find

$$\mathscr{T}_{\rm fi}^{(3c)}=\mathscr{T}_{\rm fi}^{(3a)}. \tag{14}$$

We now consider the nearly resonant diagrams and we begin by the diagram in fig. 3b. The intermediate states are $|1(N-1)\rangle\otimes|N', 1\omega_1\rangle$ and $|1(N)\rangle\otimes|(N'-1), 1\omega_1\rangle$:

$$\mathscr{T}_{\rm fi}^{(3b)}=C\frac{d_{21}^{-}d_{11}^{+}d_{12}^{-}}{[(\omega+\omega'-\omega_1-\omega_0)+\mathrm{i}\Gamma/2][(2\omega-\omega_1-\omega_0)+\mathrm{i}\Gamma/2]}. \tag{15}$$

Using eqs. (2), this yields:

$$\mathscr{T}_{\rm fi}^{(3b)}=C\left(\frac{\Omega_1}{2\delta}\right)^3\frac{d^3}{[(\omega+\omega'-\omega_1-\omega_0)+\mathrm{i}\Gamma/2][(2\omega-\omega_1-\omega_0)+\mathrm{i}\Gamma/2]}. \tag{16}$$

Because the denominators of eq. (16) can become resonant, the ratio of $\mathscr{T}_{\rm fi}^{(3b)}$ and $\mathscr{T}_{\rm fi}^{(3a)}$ (given by eq. (12)) is on the order of $\Omega_1^2/\delta\Gamma$ as stated before.

The contribution of the diagrams in figs. 3d and 3e is calculated in the appendix where it is shown that

$$\mathscr{T}_{\rm fi}^{(3d)}+\mathscr{T}_{\rm fi}^{(3e)}=\mathscr{T}_{\rm fi}^{(3b)}. \tag{17}$$

Using eqs. (14) and (17), we find that the total transition amplitude for the scattering processes involving absorption of one photon ω' and spontaneous emission of two photons ω_1 and ω_2 is:

$$\mathscr{T}_{\rm fi}^{(3a)}+\mathscr{T}_{\rm fi}^{(3b)}+\mathscr{T}_{\rm fi}^{(3c)}+\mathscr{T}_{\rm fi}^{(3d)}+\mathscr{T}_{\rm fi}^{(3e)}=2(\mathscr{T}_{\rm fi}^{(3a)}+\mathscr{T}_{\rm fi}^{(3b)}). \tag{18}$$

The physics of this scattering process should thus be understood from the interference between the nonresonant process of fig. 3a and the nearly resonant process of fig. 3b. The corresponding diagrams in the bare-atom picture are shown in fig. 4a for the nonresonant process and fig. 4b for the nearly resonant process.

From the knowledge of the transition amplitude, one can calculate the transition rate

$$\sum_{\mathrm{f}} w_{\mathrm{fi}}^{(2)} = \frac{2\pi}{\hbar} \int \frac{\mathrm{d}^3k_1\,\mathrm{d}^3k_2}{(2\pi/L)^6} \sum_{\epsilon_1} \sum_{\epsilon_2} |2(\mathscr{T}_{\mathrm{fi}}^{(3\mathrm{a})} + \mathscr{T}_{\mathrm{fi}}^{(3\mathrm{b})})|^2 \, \delta(\hbar\omega + \hbar\omega' - \hbar\omega_1 - \hbar\omega_2) \tag{19}$$

and the cross-section $\sigma_{\mathrm{abs}}^{(2)}$ by dividing $\sum_{\mathrm{f}} w_{\mathrm{fi}}^{(2)}$ by the flux $N'c/L^3$. The cross-section $\sigma_{\mathrm{abs}}^{(2)}$ is the sum of three terms. The first term $\sigma_{\mathrm{abs}}^{(\mathrm{nr})}$ comes from the contribution of the nonresonant transition amplitude $\mathscr{T}_{\mathrm{fi}}^{(3\mathrm{a})}$, the second term $\sigma_{\mathrm{abs}}^{(\mathrm{r})}$ comes from the contribution of the resonant transition amplitude $\mathscr{T}_{\mathrm{fi}}^{(3\mathrm{b})}$ and the third term $\sigma_{\mathrm{abs}}^{(\mathrm{int})}$ is associated with the interference terms involving products such as $\mathscr{T}_{\mathrm{fi}}^{(3\mathrm{a})} \mathscr{T}_{\mathrm{fi}}^{(3\mathrm{b})*}$:

$$\sigma_{\mathrm{abs}}^{(2)} = \sigma_{\mathrm{abs}}^{(\mathrm{nr})} + \sigma_{\mathrm{abs}}^{(\mathrm{r})} + \sigma_{\mathrm{abs}}^{(\mathrm{int})} . \tag{20}$$

Using eqs. (6), (7), (11), (12), (16), (19) and (20) and replacing the slowly varying functions of ω by theirs values in ω_0, one finds

$$\sigma_{\mathrm{abs}}^{(\mathrm{nr})} = \frac{3}{4\pi^2} \lambda_0^2 \left(\frac{\Omega_1}{2\delta}\right)^2 \frac{\Gamma^3}{\delta^2} \int_0^{+\infty} \frac{\mathrm{d}\omega_1}{(\omega+\omega'-\omega_1-\omega_0)^2 + \Gamma^2/4} , \tag{21a}$$

$$\sigma_{\mathrm{abs}}^{(\mathrm{r})} = \frac{3}{4\pi^2} \lambda_0^2 \left(\frac{\Omega_1}{2\delta}\right)^6 \Gamma^3 \int_0^{+\infty} \frac{\mathrm{d}\omega_1}{[(\omega+\omega'-\omega_1-\omega_0)^2 + \Gamma^2/4][(2\omega-\omega_1-\omega_0)^2 + \Gamma^2/4]} , \tag{21b}$$

$$\sigma_{\mathrm{abs}}^{(\mathrm{int})} = -\frac{3}{4\pi^2} \lambda_0^2 \left(\frac{\Omega_1}{2\delta}\right)^4 \frac{\Gamma^3}{\delta} \left(\int_0^{+\infty} \frac{\mathrm{d}\omega_1}{[(\omega+\omega'-\omega_1-\omega_0)^2 + \Gamma^2/4](2\omega-\omega_1-\omega_0-\mathrm{i}\Gamma/2)} + \mathrm{c.c.} \right) . \tag{21c}$$

The calculation of each integral is performed by replacing the lower bound 0 by $-\infty$ and using the residue theorem. This yields:

$$\sigma_{\mathrm{abs}}^{(\mathrm{nr})} = \frac{3}{2\pi} \lambda_0^2 \left(\frac{\Omega_1}{2\delta}\right)^2 \left(\frac{\Gamma}{\delta}\right)^2 , \quad \sigma_{\mathrm{abs}}^{(\mathrm{r})} = \frac{3}{\pi} \lambda_0^2 \left(\frac{\Omega_1}{2\delta}\right)^6 \frac{\Gamma^2}{\Gamma^2 + (\omega-\omega')^2} , \tag{22a,b}$$

$$\sigma_{\mathrm{abs}}^{(\mathrm{int})} = \frac{3}{\pi} \lambda_0^2 \left(\frac{\Omega_1}{2\delta}\right)^4 \frac{\Gamma^2}{\delta} \frac{\omega'-\omega}{\Gamma^2 + (\omega-\omega')^2} . \tag{22c}$$

We note that $\sigma_{\mathrm{abs}}^{(\mathrm{int})}$ can be positive or negative depending upon the sign of $(\omega-\omega')$, the total cross-section given by eq. (20) remaining of course always positive. The fact that $\sigma_{\mathrm{abs}}^{(\mathrm{int})}$ changes sign from one side of the resonance to the other indicates that on one side of the resonance, the interference between the diagrams in figs. 3a and 3b is constructive and the absorption cross-section increases. On the other side of the resonance, the interference is destructive and the absorption cross-section decreases. Similar types of interference for V [14] or Λ [15] three-level atoms have been already reported.

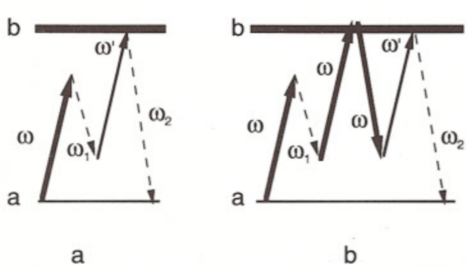

Fig. 4. Diagrammatic representation, in the bare atom basis, of some of the scattering processes represented in fig. 3. Diagrams (4a) and (4b) correspond respectively to diagrams (3a) and (3b).

We can compare each of the cross-sections given by eqs. (22) with the usual absorption cross-section given by eq. (9). The order of magnitude for $\omega'-\omega\sim\Gamma$ are

$$\sigma_{\rm abs}^{\rm (nr)}/\sigma_{\rm abs}^{(1)}=(\Omega_1/\delta)^2\,,\quad \sigma_{\rm abs}^{\rm (r)}/\sigma_{\rm abs}^{(1)}\sim(\Omega_1^2/\delta\Gamma)^2(\Omega_1/\delta)^2\,,\quad \sigma_{\rm abs}^{\rm (int)}/\sigma_{\rm abs}^{(1)}\sim(\Omega_1^2/\delta\Gamma)(\Omega_1/\delta)^2\,. \tag{23a,b,c}$$

It is clear that $\sigma_{\rm abs}^{\rm (nr)}$ is much smaller than $\sigma_{\rm abs}^{(1)}$. In contrast, the relation between $\sigma_{\rm abs}^{\rm (r)}$ and $\sigma_{\rm abs}^{(1)}$ on one hand and between $\sigma_{\rm abs}^{\rm (int)}$ and $\sigma_{\rm abs}^{(1)}$ on the other hand depend upon the value of the parameters because their ratio appears to be the product of a small parameter $(\Omega_1/\delta)^2$ by a quantity that can eventually be larger than 1. The reason why a process involving spontaneous emission of two photons may predominate over a process involving spontaneous emission of one photon is that the two-photon emission is associated with a fully-resonant diagram while the one-photon emission corresponds to a nonresonant scattering process.

Other nearly-resonant scattering processes involving the spontaneous emission of two photons with a frequency close to ω are considered in the appendix. The transition amplitude associated with these diagrams is shown to be negligible.

In conclusion, the absorption cross-section of photons ω' is the sum of the usual scattering cross-section $\sigma_{\rm abs}^{(1)}$ and of the cross-sections $\sigma_{\rm abs}^{\rm (r)}$ and $\sigma_{\rm abs}^{\rm (int)}$ which are associated with processes induced by the presence of photons ω and which display a resonance around $\omega'=\omega$.

4. Amplification of photons ω'

In the case of two-level atoms, there exist amplification processes which have a close relationship with the absorption processes. We should thus consider the amplification processes that involve the spontaneous emission of one or two photons. In fact, the amplification cross-section associated with the spontaneous emission of one photon is smaller than $\sigma_{\rm abs}^{(1)}$ by a factor on the order of $(\Omega_1/\delta)^4$ and can therefore be neglected (see appendix). Indeed, this ratio corresponds to the relative magnitude of the cross-sections associated with the processes shown in figs. (1b) and (1c) where the difference between absorption and amplification is very clear.

We now consider the processes where two spontaneous photons are emitted. We show in fig. 5, the dominant processes for amplification of photons ω' associated with the spontaneous emission of two photons with frequencies ω_1 and ω_2 close to $2\omega-\omega_0$ and ω_0, respectively. The final state of the scattering process is $|{\rm f}'\rangle=|2(N-3)\rangle\otimes|(N'+1),\,1\omega_1,\,1\omega_2\rangle$. In contrast to the case of fig. 3, the non-resonant diagrams (such as figs. 3a and 3c) should not be retained here because the matrix element $d_{\bar{1}\bar{2}}^{-}\sim d(\Omega_1/\delta)^2$ replaces the matrix element $d_{\bar{1}2}^{+}\sim d$ found in $\mathscr{T}_{\rm fi}^{(3a)}$ (eq. (10)) and $\mathscr{T}_{\rm fi}^{(3c)}$ (eq. (13)). Besides, the diagrams that involve spontaneous photons having a frequency close to ω (such that those considered in the appendix for the absorption process) interfere destructively.

The three diagrams in fig. 5 are nearly resonant. The transition amplitude for the diagram in fig. 5a is

$$\mathscr{T}_{\rm fi}^{(5a)}=C'\frac{d_{\bar{2}1}^{-}d_{\bar{1}1}^{-}d_{\bar{1}2}^{-}}{[(3\omega-\omega'-\omega_1-\omega_0)+{\rm i}\Gamma/2][(2\omega-\omega_1-\omega_0)+{\rm i}\Gamma/2]}\,, \tag{24}$$

with

$$C'=-{\rm i}\frac{\sqrt{\omega'\omega_1\omega_2}\sqrt{N'+1}}{(2\epsilon_0L^3)^{3/2}\sqrt{\hbar}}\,\epsilon_{1z}\epsilon_{2z}\,. \tag{25}$$

Comparing eqs. (24) and (25) with eqs. (15) and (11), using $\sqrt{N'+1}\approx\sqrt{N'}$ and $d_{\bar{1}1}^{+}=d_{\bar{1}1}^{-}$ and writing the energy denominators as a function of the independent variables ω and $\omega'-\omega$, one finds

$$\mathscr{T}_{\rm fi}^{(5a)}(\omega'-\omega)=-\mathscr{T}_{\rm fi}^{(3b)}(\omega-\omega')\,. \tag{26}$$

Similar equations can be obtained for the other transition amplitudes:

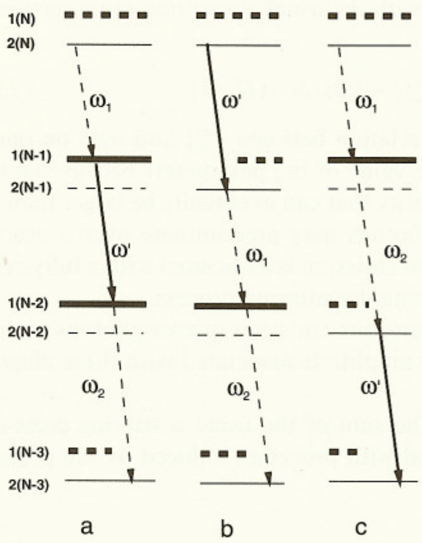

Fig. 5. Diagrammatic representation of the dominant scattering processes, involving two fluorescence photons ω_1 and ω_2 (with $\omega_1 \approx 2\omega - \omega_0$ and $\omega_2 \approx \omega_0$), and responsible for the amplification of the probe field for $\omega' \approx \omega$. The conventions are the same as for fig. 2. For each of the three diagrams, all intermediate states are nearly resonant. The diagrams containing one non resonant intermediate state may be shown to have a negligible contribution.

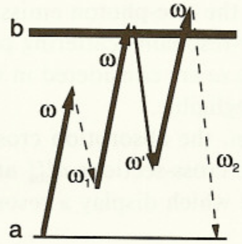

Fig. 6. Diagrammatic representation, in the bare atom basis, of the scattering process represented in fig. 5a.

$$\mathscr{T}_{\mathrm{fi}}^{(5\mathrm{b})}(\omega'-\omega) = -\mathscr{T}_{\mathrm{fi}}^{(3\mathrm{d})}(\omega-\omega')\,, \quad \mathscr{T}_{\mathrm{fi}}^{(5\mathrm{c})}(\omega'-\omega) = -\mathscr{T}_{\mathrm{fi}}^{(3\mathrm{e})}(\omega-\omega')\,. \tag{27a,b}$$

Using eqs. (17) and (26), one then obtains

$$\mathscr{T}_{\mathrm{fi}}^{(5\mathrm{b})} + \mathscr{T}_{\mathrm{fi}}^{(5\mathrm{c})} = \mathscr{T}_{\mathrm{fi}}^{(5\mathrm{a})}\,, \tag{28}$$

which shows that the knowledge of $\mathscr{T}_{\mathrm{fi}}^{(5\mathrm{a})}$ is sufficient for calculating the amplification cross-section. The diagram which corresponds to fig. 5a is shown in fig. 6 in the bare-atom basis.

The amplification cross-section can be calculated starting from a formula identical to eq. (19) where $\mathscr{T}_{\mathrm{fi}}^{(3\mathrm{a})} + \mathscr{T}_{\mathrm{fi}}^{(3\mathrm{b})}$ is replaced by $\mathscr{T}_{\mathrm{fi}}^{(5\mathrm{a})}$. In fact, because of the equality (26), the amplification cross-section $\sigma_{\mathrm{amp}}^{(2)}(\omega-\omega')$ is just equal to the contribution $\sigma_{\mathrm{abs}}^{(\mathrm{r})}(\omega'-\omega)$ of the resonant transition amplitudes to $\sigma_{\mathrm{abs}}^{(2)}$. Furthermore, because $\sigma_{\mathrm{abs}}^{(\mathrm{r})}(\omega'-\omega)$ is an even function of $(\omega-\omega')$ (given by eq. (22b)), this yields:

$$\sigma_{\mathrm{amp}}^{(2)} = \sigma_{\mathrm{abs}}^{(\mathrm{r})}\,. \tag{29}$$

The equality between these cross-sections is particularly clear in the bare-atom picture. The Raman process of fig. 6 just balances the Raman process of fig. 4b because on one hand the same transitions are involved and the other hand the initial and final states coïncide in both cases with the atomic ground state.

5. Competition between absorption and amplification

In the limit considered in this paper, the total absorption cross-section σ_{abs} results from the processes considered in sections 3.1, 3.2 and 4:

$$\sigma_{\mathrm{abs}}=\sigma_{\mathrm{abs}}^{(1)}+\sigma_{\mathrm{abs}}^{(2)}-\sigma_{\mathrm{amp}}^{(2)} . \tag{30}$$

From eqs. (20) and (29), we find

$$\sigma_{\mathrm{abs}}=\sigma_{\mathrm{abs}}^{(1)}+\sigma_{\mathrm{abs}}^{(\mathrm{int})} , \tag{31}$$

because we have shown that $\sigma_{\mathrm{abs}}^{(\mathrm{nr})} \ll \sigma_{\mathrm{abs}}^{(1)}$. Using eqs. (9) and (22c), we finally obtain

$$\sigma_{\mathrm{abs}}=\frac{3}{8\pi}\lambda_0^2\left(\frac{\Gamma}{\delta}\right)^2\left[1+\frac{\Omega_1^4}{2\delta^3}\frac{\omega'-\omega}{\Gamma^2+(\omega-\omega')^2}\right]. \tag{32}$$

This expression coincides with the leading terms of the expansion of σ_{abs} obtained from the exact expression [7]. In particular, it predicts that σ_{abs} can become negative, i.e. that amplification is possible when $\Omega_1^4 > 4|\delta|^3\Gamma$, a condition which was derived in ref. [8]. When this condition is fulfilled, the resonant scattering processes of fig. 3b is so large that its interference with the small non resonant contribution of fig. 3a can be larger than the losses due to Rayleigh scattering given by eq. (9).

It is worth emphasizing the origin of the amplification. The absorption and gain processes shown in figs. 4b and 6 lead to exactly opposite effects. This equilibrium is broken by the interference occurring on the absorption between the diagrams in figs. 4a and 4b. In particular, when $\delta(\omega'-\omega)<0$, the absorption is weakened so that amplification may be achieved.

For the processes considered here, amplification is not associated with any population inversion both in the bare state basis and in the dressed state basis. In the bare state basis, the Raman processes start and end in the ground state (see figs. 4 and 6). In the dressed-state basis, the transition occurs between two levels $|2(N_1)\rangle$ and $|2(N_2)\rangle$ which have exactly the same population. Here the origin of amplification is really associated with a weakening of absorption due to a destructive interference between several processes.

6. Conclusion

All the results described in this paper for the case of radiative damping can be extended to other damping mechanisms and in particular to collisional relaxation. For example, diagrams analogous to those shown in figs. 4a and 4b and yielding collisionally-aided absorption are shown in figs. 7a and 7b. Here again, these two diagrams can interfere leading to an increase or a decrease of the absorption depending on the sign of $(\omega'-\omega)$ [14]. One should of course add to these absorption processes the usual elastic scattering considered in subsection 3.1. The collisionally-aided gain process analogous to the process of fig. 6 is shown in fig. 7c. Here again, in the absence of interference on the absorption, the collisionally-aided gain of fig. 7c would be balanced by the collisionally-aided absorption of fig. 7b. However the interference can be sufficiently large to break this symmetry and to yield an amplification which was sufficient to observe a laser oscillation with sodium atoms [10].

The approach that we present here is important, not only because it provides a better understanding of a phenomenon which was known for years, but also because it provides the possibility to imagine new lasers without population inversion. In the diagrams shown in fig. 7, we can, for instance, replace the one-photon processes involving the field ω by two-photon processes provided that levels b and a can be coupled by one- and two-photon transitions (that can be done by applying a static electric field). For a sufficiently large value of the pump field, the destructive interference that occurs between the diagrams of figs. 7a and 8a on one side of the resonance $2\omega=\omega'$ allows the Raman gain of fig. 8b to become dominant. A laser emission occurring near $\omega'=2\omega$ is then possible. It is important to note that this process is very different from harmonic generation. The maximum gain will not occur for $\omega'=2\omega$ but for $|\omega'-2\omega| \sim \Gamma$. Furthermore, the phase-matching condition $(\boldsymbol{k}'=2\boldsymbol{k})$, which is of fundamental importance for harmonic generation because the second harmonic originates from the coherent superposition of the fields radiated by all the electric dipole moments in the sam-

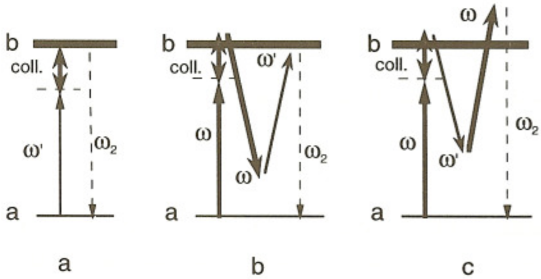

Fig. 7. Collisionally-aided processes leading to an absorption or an amplification of the probe field ω'. The double arrow represents the energy provided by the collision. Diagrams (a) and (b) describe absorption processes which are analogous to those represented in figs. 4a and 4b, respectively. Diagram (c) describes an amplification of the field ω' analogous to the process represented in fig. 6. Here again, the interference between the amplitudes associated with diagrams (a) and (b) breaks the balance between the absorption and the amplification amplitudes associated with diagrams (b) and (c).

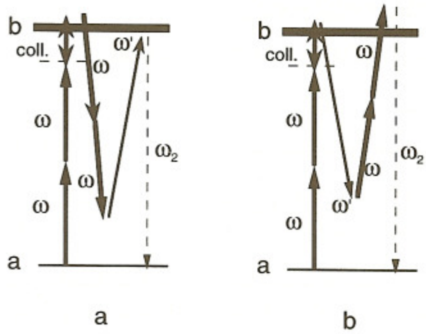

Fig. 8. Collisionally-aided processes leading to an absorption or an amplification of the probe field ω' and involving the absorption or the emission of pairs of pump photons ω. The conventions are the same as for fig. 7. Levels a and b have not a well defined parity so that they can be connected by one-photon or two-photon transitions. Here again, the interference between the amplitudes associated with the diagrams of fig. 7a and fig. 8a can break the balance between the absorption and the amplification amplitudes associated with the diagrams of (a) (b).

ple, has a much weaker importance for the process described here because this process corresponds to an amplification mechanism. In fact, for stationary atoms the absorption coefficient (given by an equation similar to eq. (32)) is even independent of $(\boldsymbol{k}'-2\boldsymbol{k})$. This factor only appears for moving atoms because the replacement of ω by $\omega-\boldsymbol{k}\cdot\boldsymbol{v}$ and ω' by $\omega'-\boldsymbol{k}'\cdot\boldsymbol{v}$ and the averaging over the velocity distribution leads to a residual Doppler effect depending on $(\boldsymbol{k}'-2\boldsymbol{k})$. These points (position of the resonance, phase-matching conditions) show clearly the difference between harmonic generation and the gain mechanism described here.

Appendix

We specify in this Appendix some of the results that have been presented without any demonstration precedently.

We first consider the three diagrams shown in figs. 2b–d and show that their contribution to the absorption cross-section is negligible compared to that of the diagram in fig. 2a. The diagram of fig. 2b corresponds to a process where the photon ω_1 is emitted before the photon ω' is absorbed, the intermediate state being $|1(N-1)\rangle\otimes|N', 1\omega_1\rangle$. The corresponding transition amplitude is

$$\mathscr{T}_{\mathrm{fi}}^{(2\mathrm{b})}=\frac{\sqrt{\omega'\omega_1}}{2\epsilon_0 L^3}\sqrt{N'}\,\epsilon_{1z}\frac{d_{21}^{+}d_{12}^{-}}{2\delta-\delta'+\mathrm{i}\Gamma/2}\,. \tag{A.1}$$

Each of the matrix element $d_{ij}^{\pm}$ of eq. (A.1) is on the order of $d(\Omega_1^2/\delta^2)$ (see eq. (2d)). The energy denominator of eq. (A.1) being on the same order of magnitude as the one of eq. (3) because we have assumed that $|\delta-\delta'|\ll|\delta|$, we conclude that

$$\mathscr{T}_{\mathrm{fi}}^{(2\mathrm{b})}\sim(\Omega_1^4/\delta^4)\,\mathscr{T}_{\mathrm{fi}}^{(2\mathrm{a})}\,, \tag{A.2}$$

$\mathscr{T}_{\mathrm{fi}}^{(2\mathrm{b})}$ can thus be neglected. We now consider the diagrams of figs. 2c and 2d. These diagrams involve as intermediate states $|2(N+1)\rangle \otimes |(N'-1), 0\rangle$ and $|2(N-1)\rangle \otimes |N', 1\omega_1\rangle$, respectively. The transition amplitudes for these diagrams are

$$\mathcal{T}_{\mathrm{fi}}^{(2\mathrm{c})} \approx \frac{\sqrt{\omega'\omega_1}}{2\epsilon_0 L^3} \sqrt{N'}\, \epsilon_{1z} \frac{d_{22}^{-} d_{22}^{+}}{\omega' - \omega}, \quad \mathcal{T}_{\mathrm{fi}}^{(2\mathrm{d})} \approx \frac{\sqrt{\omega'\omega_1}}{2\epsilon_0 L^3} \sqrt{N'}\, \epsilon_{1z} \frac{d_{22}^{+} d_{22}^{-}}{\omega - \omega'}. \tag{A.3a,b}$$

It clearly appears that

$$\mathcal{T}_{\mathrm{fi}}^{(2\mathrm{c})} + \mathcal{T}_{\mathrm{fi}}^{(2\mathrm{d})} \approx 0 . \tag{A.4}$$

The two diagrams shown in figs. 2c and 2d have an opposite amplitude so that their global contribution to the scattering process is zero. In the dressed-state basis the processes involving the absorption of one photon ω' and the emission of one fluorescence photon is thus described entirely (at the lowest order in Ω_1/δ) by the diagram of fig. 2a.

We now consider the diagrams describing absorption of photon ω' and involving spontaneous emission of two photons. We first study the relation between the diagrams in figs. 3b, d and e. The diagram in fig. 3d has intermediate states equal to $|2(N+1)\rangle \otimes |(N'-1), 0\rangle$ and $|1(N)\rangle \otimes |(N'-1), 1\omega_1\rangle$:

$$\mathcal{T}_{\mathrm{fi}}^{(3\mathrm{d})} \approx C \frac{d_{21}^{-} d_{12}^{-} d_{22}^{+}}{[(\omega+\omega'-\omega_1-\omega_0)+\mathrm{i}\Gamma/2](\omega'-\omega)}. \tag{A.5}$$

Using eqs. (2), we find

$$\mathcal{T}_{\mathrm{fi}}^{(3\mathrm{d})} \approx -C \left(\frac{\Omega_1}{2\delta}\right)^3 \frac{d^3}{[(\omega+\omega'-\omega_1-\omega_0)+\mathrm{i}\Gamma/2](\omega'-\omega)}. \tag{A.6}$$

The intermediate states for the diagram in fig. 3e are $|1(N-1)\rangle \otimes |N', 1\omega_1\rangle$ and $|2(N-2)\rangle \otimes |N', 1\omega_1, 1\omega_2\rangle$:

$$\mathcal{T}_{\mathrm{fi}}^{(3\mathrm{e})} \approx C \frac{d_{22}^{+} d_{21}^{-} d_{12}^{-}}{[(2\omega-\omega_1-\omega_2)][(2\omega-\omega_1-\omega_0)+\mathrm{i}\Gamma/2]}, \tag{A.7}$$

The energies of the initial state $|\mathrm{i}\rangle$ and of the final state $|\mathrm{f}\rangle$ being equal, we have $\omega+\omega'=\omega_1+\omega_2$. It follows that $(2\omega-\omega_1-\omega_2)=(\omega-\omega')$. Using eqs. (2), we get

$$\mathcal{T}_{\mathrm{fi}}^{(3\mathrm{e})} \approx -C \left(\frac{\Omega_1}{2\delta}\right)^3 \frac{d^3}{(\omega-\omega')[(2\omega-\omega_1-\omega_0)+\mathrm{i}\Gamma/2]}. \tag{A.8}$$

A simplification occurs if one sums $\mathcal{T}_{\mathrm{fi}}^{(3\mathrm{d})}$ and $\mathcal{T}_{\mathrm{fi}}^{(3\mathrm{e})}$. From eqs. (A.6) and (A.8), we deduce

$$\mathcal{T}_{\mathrm{fi}}^{(3\mathrm{d})} + \mathcal{T}_{\mathrm{fi}}^{(3\mathrm{e})} \approx C \left(\frac{\Omega_1}{2\delta}\right)^3 \frac{d^3}{[(\omega+\omega'-\omega_1-\omega_0)+\mathrm{i}\Gamma/2][(2\omega-\omega_1-\omega_0)+\mathrm{i}\Gamma/2]} \tag{A.9}$$

Comparing this expression with eq. (16), we find eq. (17).

Other nearly-resonant scattering processes involving the emission of two photons are possible, these two photons having frequencies ω_1 and ω_2 close to ω. Diagrams associated with this type of process are shown in fig. 9. It is possible to show that these processes do not contribute to the absorption cross-section for photons ω' because the sum of the transition amplitudes associated with those nearly resonant scattering processes is equal to 0. More precisely, each of the transition amplitude of the diagrams in fig. 9 can be calculated as it was done before for the diagrams in figs. 2 and 3 and one obtains

$$\mathcal{T}_{\mathrm{fi}}^{(9\mathrm{a})} + \mathcal{T}_{\mathrm{fi}}^{(9\mathrm{b})} + \mathcal{T}_{\mathrm{fi}}^{(9\mathrm{c})} = 0 . \tag{A.10}$$

Finally, it turns out that the dominant nearly-resonant scattering processes are described by the diagrams in figs. 3b, d and e and that the contribution of these diagrams can be larger than the usual absorption process shown in fig. 2a. Because a scattering process involving the spontaneous emission of two photons may be larger

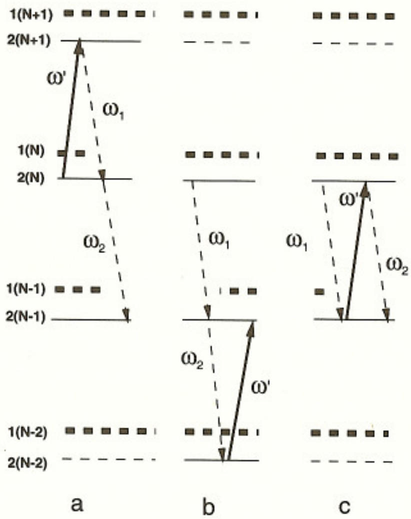

Fig. 9. Diagrammatic representation of scattering processes involving two fluorescence photons ω_1 and ω_2 (with $\omega_1 \approx \omega$, $\omega_2 \approx \omega$), and responsible for the absorption of the probe field for $\omega' \approx \omega$. The conventions are the same as for fig. 2. The sum of the amplitudes associated with the three diagrams (a), (b), (c), may be shown to be equal to zero.

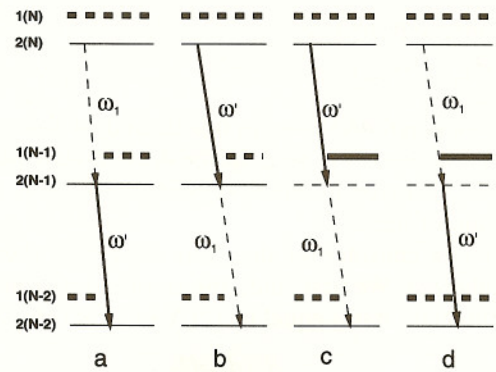

Fig. 10. Diagrammatic representation of scattering processes involving one fluorescence photon ω_1 and responsible for the amplification of the probe field ω' for $\omega' \approx \omega$. The conventions are the same as for fig. 2.

than scattering processes where only one photon is emitted, one may wonder if it would not be necessary to consider terms with three, four, ..., emitted photons. This is not the case. For example, the comparison of fig. 3c with fig. 2a shows that fig. 3c has an additional step which is resonant. However, the cross-section associated with fig. 3c is smaller than the one associated with fig. 2a by a factor $(\Omega_1/\delta)^2$ (see eq. (22a)). Actually, for each nearly-resonant photon added to a given diagram, the cross-section is multiplied by a factor on the order of $(1/\Gamma)^2(d_{ij}/d)^2\Gamma^2$. The first factor $(1/\Gamma)^2$ comes from the new resonant denominator in the transition amplitude, $(d_{ij})^2$ arises from the new matrix element of the dipole moment appearing in the transition amplitude. (Γ/d^2) is a constant and a final Γ appears from the integration of the energy of the spontaneous photon. In conclusion, each time a new resonant spontaneous photon is emitted, the cross-section decreases by a factor $(d_{ij}/d)^2$. The transition from a two-photon emission to a three-photon emission implies that d_{ij} is $d_{\bar{1}\bar{1}}$ or $d_{\bar{2}\bar{2}}$. The corresponding cross-section is then reduced by a factor $(\Omega_1/\delta)^2$. The transition from a two-photon emission to a four-photon emission needs either two $d_{\bar{i}\bar{i}}$ or a $d_{\bar{1}\bar{2}}$ and a $d_{\bar{2}\bar{1}}$. In both cases, the corresponding cross-section is reduced by a factor $(\Omega_1/\delta)^4$.

We finally consider the diagrams describing amplification of the field ω' and we calculate the processes where only one spontaneous photon is emitted (the processes involving spontaneous emission of two photons are described and calculated in sect. 4). The final state of a process involving amplification of photons ω' and spontaneous emission of one photon ω_1 (fig. 10) is $|\mathrm{f}\rangle = |2(N-2)\rangle \otimes |(N'+1), 1\omega_1\rangle$. First we note that the two diagrams shown in figs. 10a and 10b in which the intermediate state has a $|2(N-1)\rangle$ component interfere destructively (the calculation is similar to the one done for the diagrams in fig. 2c and 2d):

$$\mathcal{T}_{\mathrm{fi}}^{(10\mathrm{a})} + \mathcal{T}_{\mathrm{fi}}^{(10\mathrm{b})} = 0 .$$

The two diagrams shown in figs. 10c and 10d are nearly equal. Replacing $2\omega - \omega_0 - \omega'$ by δ (because $\omega \approx \omega'$), one obtains

$$\mathcal{T}_{\mathrm{fi}}^{(10\mathrm{c})} = \mathcal{T}_{\mathrm{fi}}^{(10\mathrm{d})} = \frac{\sqrt{\omega'\omega_1'}}{2\epsilon_0 L^3}\sqrt{N'+1}\,\epsilon_{1z}\frac{d_{21}^{-}d_{12}^{-}}{\delta+\mathrm{i}\Gamma/2} \tag{A.11}$$

Because d_{12}^{-} is smaller than d_{12}^{+} by a factor $(\Omega_1/2\delta)^2$, the comparison between eq. (A.11) and eq. (3b) shows that

$$\mathcal{T}_{\mathrm{fi}}^{(10\mathrm{c})} = \mathcal{T}_{\mathrm{fi}}^{(10\mathrm{d})} \sim (\Omega_1/2\delta)^2 \mathcal{T}_{\mathrm{fi}}^{(2\mathrm{a})} \,. \tag{A.12}$$

The amplification cross-section associated with the diagrams in fig. 10 is thus smaller than the absorption cross-section $\sigma_{\mathrm{abs}}^{(1)}$ given by eq. (9) by a factor on the order of $(\Omega_1/\delta)^4$ and can therefore be neglected. In fact, one may consider the diagram in fig. 10c to be the wing of the amplification process described in fig. 1c in the bare state basis.

References

[1] B.R. Mollow, Phys. Rev. A 5 (1972) 2217.
[2] F.Y. Wu, S. Ezekiel, M. Ducloy and B.R. Mollow, Phys. Rev. Lett. 38 (1977) 1077.
[3] G. Grynberg, F. Biraben, M. Bassini and B. Cagnac, Phys. Rev. Lett. 37 (1976) 283.
[4] C. Cohen-Tannoudji and S. Reynaud, J. Phys. B 10 (1977) 345;
G. Khitrova, J.F. Valley and H.M. Gibbs, Phys. Rev. Lett. 60 (1988) 1126;
A. Lezama, Y. Zhu, M. Kanskar and T.W. Mossberg, Phys. Rev. A 41 (1990) 1576;
G.S. Agarwal, Phys. Rev. A 42 (1990) 686.
[5] G.S. Agarwal and N. Nayak, J. Opt. Soc. Am. B 1 (1984) 164;
P.R. Berman, G. Khitrova and J.F. Lam, in: Spectral line shapes, vol. 3, ed. F. Rostas (Gruyter, Berlin, 1985) p. 337;
H. Friedman and A.D. Wilson-Gordon in: Methods in laser spectroscopy, eds. Y. Prior, A. Ben-Reuven and M. Rosenbluh (Plenum, New-York, 1986) p. 307.
[6] M.T. Gruneisen, K.R. MacDonald and R.W. Boyd, J. Opt. Soc. Am. B 5 (1988) 123.
[7] M. Pinard and G. Grynberg, J. Phys. (France) 49 (1988) 2027.
[8] G. Grynberg, E. Le Bihan and M. Pinard, J. Phys. (France) 47 (1986) 1321.
[9] G. Grynberg and P.R. Berman, Phys. Rev. A 39 (1989) 4016.
[10] D. Grand Clement, G. Grynberg and M. Pinard, Phys. Rev. Lett. 59 (1987) 40;
J. Zakrzewski, Phys. Rev. A submitted.
[11] C. Cohen-Tannoudji, J. Dupont-Roc and G. Grynberg, Atom-photon interactions (Wiley, New York, 1992).
[12] O. Kocharovskaya and Yu. I. Khanin, JETP 48 (1988) 581;
S.E. Harris, Phys. Rev. Lett. 62 (1989) 1033;
M.O. Scully, S.Y. Zhu and A. Gavrielides, Phys. Rev. Lett. 62 (1989) 2813;
G.S. Agarwal, S. Ravi and J. Cooper, Phys. Rev. A 41 (1990) 4721, 4727;
O. Kocharovskaya and P. Mandel, Phys. Rev. A 42 (1990) 523;
A. Imamoglu, J.E. Field and S.E. Harris, Phys. Rev. Lett. 66 (1991) 1154;
L.M. Narducci, H.M. Doss, P. Ru, M.O. Scully, S.Y. Zhu and C. Keitel, Optics Comm. 81 (1991) 379.
[13] C. Cohen-Tannoudji, J. Dupont-Roc and G. Grynberg, Photons and atoms, (Wiley, New York, 1989) p. 325.
[14] G. Grynberg and P.R. Berman, Phys. Rev. A 41 (1990) 2677; A 43 (1991) 3994.
[15] B. Lounis and C. Cohen-Tannoudji, J. Phys. II (France) 2 (1992) 579.